Biochemistry

pubs.acs.org/biochemistry Article

Oligomeric Changes Regulate Flavin Transfer in Two-Component FMN Reductases Involved in Sulfur Metabolism

Chioma H. Aloh, Tonya N. Zeczycki, and Holly R. Ellis*

Cite This: *Biochemistry* 2023, 62, 2751−2762 Read Online

ACCESS | Metrics & More | Article Recommendations | Supporting Information

ABSTRACT: The FMN reductases (SsuE and MsuE of the alkanesulfonate monooxygenase systems) supply reduced flavin to their partner monooxygenases for the desulfonation of alkanesulfonates. Flavin reductases that comprise two-component systems must be able to regulate both flavin reduction and transfer. One mechanism to control these distinct processes is through changes in the oligomeric state of the enzymes. Despite their similar overall structures, SsuE and MsuE showed clear differences in their oligomeric states in the presence of substrates. The oligomeric state of SsuE was converted from a tetramer to a dimer/tetramer equilibrium in the presence of FMN or NADPH in analytical ultracentrifugation studies. Conversely, MsuE shifted from a dimer to a single tetrameric state with FMN, and the NADPH substrate did not induce a similar oligomeric shift. There was a fast tetramer to dimer equilibrium shift occurring at the dimer/dimer interface in H/D-X investigations with apo SsuE. Formation of the SsuE/FMN complex slowed the tetramer/dimer conversion, leading to a slower exchange along the dimer/dimer interface. The oligomeric shift of the MsuE/FMN complex from a dimer to a distinct tetramer showed a decrease in H/D-X in the region around the π-helices at the dimer/dimer interface. Both SsuE and MsuE showed a comparable and significant increase in the melting temperature with the addition of FMN, indicating the conformers formed by each FMN-bound enzyme had increased stability. A mechanism that supports the different structural shifts is rationalized by the different roles these enzymes play in providing reduced flavin to single or multiple monooxygenase enzymes.

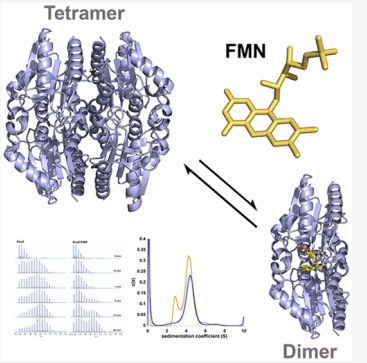

INTRODUCTION

Sulfur plays a key role as a component of metabolites needed for the survival of organisms. For bacteria, inorganic sulfate is often limiting in the environment and alternate organosulfur compounds are utilized for sulfur assimilation.[1,2] Some organosulfur sources that bacteria use under sulfur-limiting conditions include alkanesulfonates, aryl sulfonates, aromatic sulfonates, and sulfate esters.[3] The alkanesulfonate monooxygenase system is expressed in a diverse group of bacteria and is comprised of a NADPH-dependent FMN reductase (SsuE), a $FMNH_2$-dependent alkanesulfonate monooxygenase (SsuD), and transport proteins that catalyze the transport and desulfonation of alkanesulfonates (Scheme 1A).[4−6] In addition to the alkanesulfonate monooxygenase enzymes, some organisms express the methanesulfinate monooxygenase operon that encodes a flavin-dependent reductase (MsuE) and two structurally distinct monooxygenases (MsuC/MsuD) that together convert methanesulfinate to formaldehyde and sulfite in consecutive reactions (Scheme 1B).[7−9] In both systems, flavin reduction by the FMN reductase and reduced flavin transfer to the monooxygenase must be coordinated between the enzymes for the desulfonation reaction to be successful (Scheme 1).

The two-component flavin reductases involved in sulfur acquisition belong to the NADPH-dependent FMN reductase family. Members of the family have a flavodoxin fold and consist of both canonical flavin reductases with a tightly bound flavin and FMN-dependent reductases with a monooxygenase partner that utilizes flavin as a substrate. A distinct structural difference between these two groups within the family is the presence of a π-helix located at the dimer/dimer interface of the FMN-dependent reductases.[10] The π-helix is often contained within a conserved alpha helix and has $i + 5$ intrastrand hydrogen bonding, resulting in a wide turn and increased flexibility.[11,12] This altered helical structure provides a gain-of-function for enzymes outside of the structural and catalytic properties of the enzyme family.[13] Given the functional difference between the two groups within the NADPH-dependent FMN reductase family, the π-helix has been proposed to play a role in providing a mechanism for flavin release and subsequent transfer to the monooxygenase enzymes. In previous studies, SsuE was not able to transfer flavin to the SsuD monooxygenase when the π-helix was altered to an α-helix, and the FMN-bound variant had similar

Received: July 12, 2023
Revised: August 15, 2023
Published: August 31, 2023

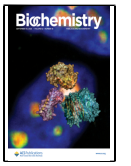

https://doi.org/10.1021/acs.biochem.3c00361
Biochemistry 2023, 62, 2751−2762

Scheme 1. Reactions Catalyzed by the Alkanesulfonate Monooxygenase Enzymes

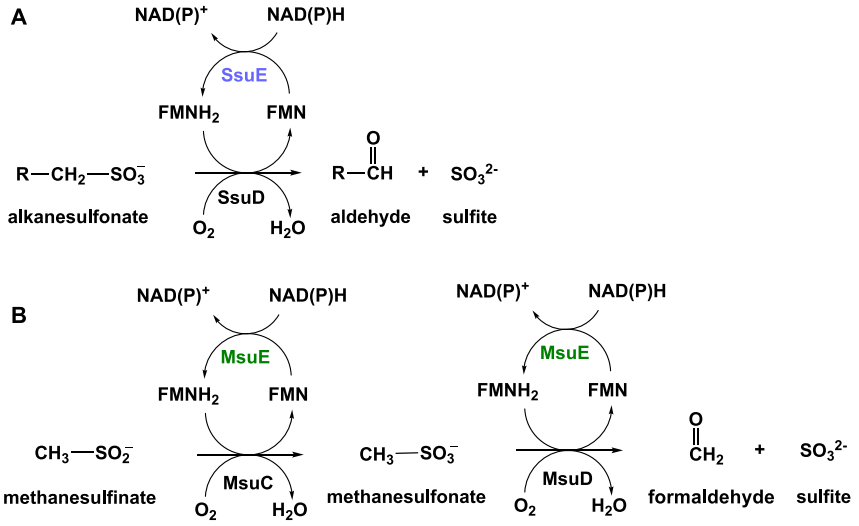

catalytic properties as canonical flavoproteins within the family.[12] MsuE (PDB: 4C76) also contains a π-helix in a comparable structural orientation as SsuE.

Reduced flavin is prone to autooxidation in the presence of oxygen so a transfer mechanism that prevents the production of reactive oxygen species is favored. In several two-component flavin-dependent systems, reduced flavin transfer involves protein−protein interactions between the FMN reductase and monooxygenase.[14−19] Flavin transfer in the alkanesulfonate monooxygenase system is dependent on protein−protein interactions, and these interaction sites are located at the dimer/dimer interface of SsuE that includes the π-helix.[16,17] Interestingly, different oligomeric states have been observed for SsuE depending on the protocol and/or conditions employed to evaluate the structure.[4,10] A switch in oligomeric states promoted by the π-helix would expose the protein−protein interaction sites and may serve as a regulation mechanism for enzyme activity and/or flavin transfer. The FMN reductases (SsuE and MsuE) in the alkanesulfonate monooxygenase systems have a similar overall structure and share about 30% amino acid identity.[10] Therefore, these enzymes may utilize a similar mechanism for flavin reduction and transfer.

The mechanisms that trigger oligomeric changes in SsuE have not been clearly defined.[10] In addition, there have been no studies to evaluate if changes in the oligomeric states of MsuE occur in the methanesulfinate/methanesulfonate system. Because MsuE provides reduced flavin to two different monooxygenase enzymes, oligomeric changes could regulate reduced flavin transfer to each monooxygenase. The studies described herein were carried out to firmly establish the oligomeric state of SsuE and MsuE with and without substrates (FMN and NADPH) and identify if these enzymes share similar oligomeric alterations. This detailed evaluation of oligomeric states is critical to understanding how structural changes are involved in the overall mechanism of the alkanesulfonate monooxygenase system. The results reported here provide the first detailed insights into the mechanisms that facilitate oligomeric changes of the FMN reductases (SsuE/MsuE) to promote protein−protein interactions and flavin transfer.

EXPERIMENTAL PROCEDURES

Materials. All reagents were purchased from Sigma-Aldrich, Biorad, or Fisher. The *SsuE* and *MsuE* genes were cloned separately into the RNA polymerase-dependent vector pET21a (Novagen) and expressed in *Escherichia coli* BL21 (DE3), as previously described.[20,21] The concentrations of SsuE and MsuE in solution were calculated with the molar extinction coefficient of each protein (20.3 and 7.4 mM^{-1} cm^{-1}).[20,21]

Non-denaturing Polyacrylamide Gel Electrophoresis. Native-PAGE experiments were carried out with SsuE and MsuE in the presence and absence of FMN to perform an initial evaluation of the oligomeric states of each enzyme. The gel was composed of a 5% stacking gel, 12% resolving gel, and tris-glycine buffer without SDS. Aliquots of the reductases, SsuE and MsuE (20 μM), were separated in the apo form and with substrates. When substrates were included, flavin (100 μM) or NADPH (500 μM) was added to 20 μM SsuE or MsuE, and the samples were mixed with native sample buffer to a total volume of 15 μL. The gels were run at a constant voltage of 120 V for 8 h at 4 °C. Protein bands were visualized using Coomassie brilliant blue staining, and the molecular weight of protein samples was compared to the stokes radius of native gel protein standards. The native gels were imaged under ultraviolet light using a ChemiDocTM MP imaging system.

Spectrofluorimetric Titrations. All fluorescence spectroscopy measurements were recorded at room temperature using a spectrofluorophotometer RF-6000 (Shimadzu) in a 10 mm quartz cuvette with the excitation slit width set at 3 nm and the emission slit width set at 5 nm. Aliquots (1 μL) of FMN (0.04−0.4 μM) or FAD (6−120 μM) were titrated into a 1 mL solution of SsuE (0.4 μM) in 25 mM potassium phosphate buffer (pH 7.5) and 100 mM NaCl. Fluorescent intensity was measured at an emission wavelength of 342 nm and an excitation wavelength of 280 nm. Because of the absence of Trp residues in MsuE, the binding affinity of MsuE for FMN was determined by monitoring the decrease in the relative fluorescence intensity of FMN due to flavin quenching on binding to MsuE. MsuE (0.02−0.4 μM, 1 μL aliquots) was titrated into a 1 mL solution of 0.1 μM FMN or 10 μM FAD in 25 mM phosphate (pH 7.5) and 100 mM NaCl. Emission

https://doi.org/10.1021/acs.biochem.3c00361
Biochemistry 2023, 62, 2751−2762

wavelengths at 525 nm were monitored using an excitation wavelength of 450 nm.

The binding affinity of pyridine nucleotides to SsuE and MsuE was also investigated through spectrofluorimetric titrations. SsuE (0.4 μM) in 1 mL 25 mM phosphate (pH 7.5), 100 mM NaCl was titrated with NADPH or NADH (10−200 μM) for a total of 20 additions. The binding of pyridine nucleotides to MsuE was measured by monitoring the increase in pyridine nucleotide fluorescence intensity upon addition of NADPH or NADH (10−200 μM, 1 μL aliquots) to MsuE (1 μM). Emission wavelengths at 450 nm for NADPH or NADH binding to SsuE or MsuE were monitored using an excitation wavelength of 340 nm. All experiments were carried out in triplicate, and the fluorescence spectra were measured after a 2 min incubation to reach equilibrium after each addition of titrant. The [ES] bound was calculated as previously described and plotted against the free substrate or enzyme concentration.[20] All plots were fitted with the quadratic equation to obtain the dissociation constant (K_d).

Thermal Melt Circular Dichroism Spectroscopy. Circular dichroism (CD) spectroscopy measurements as a function of both temperature and wavelength were utilized to monitor the thermal stability of SsuE and MsuE using a Chirascan V-100 (Applied Photophysics UK). The temperature was increased at a step interval of 2 °C using a peltier-controlled temperature cell holder (Quantum North-West). The thermal melting was measured at a heating rate of 2 °C/min. SsuE and MsuE at a concentration of 5 μM in 10 mM potassium phosphate (pH 7.5), respectively, were placed in a sealed quartz cuvette of 0.5 mm pathlength, and a temperature probe was immersed in the cuvette. The change in absorbance was scanned over a wavelength range of 185−300 nm and a temperature range of 20−94 °C. The thermal stability of each protein was also evaluated in the presence of FMN (enzyme, 5 μM: FMN, 50 μM) and NADPH (enzyme, 2 μM: NADPH, 100 μM) for each reductase. All experiments were carried out in triplicate.

The CD thermal melting profiles were analyzed using Global3 software (v. 3.1.0.78, Applied Photophysics). A plot of absorbance vs wavelength gives an unfolding curve for each temperature. Each melting curve is fitted with a sigmoidal function, which is derived from the Gibbs−Helmholtz equation:

$$\mathrm{CD}(T) = \frac{(m_F T + b_F) - (m_U T + b_U)}{1 + e^{\Delta H_{vH}/R}(1/T_m - 1/T)} + m_U T + b_U q \quad (1)$$

This equation comprises both local and global fitting variables. The thermodynamic parameters, melting temperature T_m and van't Hoff's enthalpy ΔH_{vH}, are global variables which are consistent for each wavelength. The local fitting parameters, b_F and b_U describes CD signals corresponding to the completely folded and unfolded conformation of the protein at a certain wavelength. The m_F and m_U variables stand for baseline at pre- and post-transition regions when baseline correction (single-baseline or double-baseline correction) is required. In the equation, T describes the absolute temperature and R is the gas constant (8.314 J/mol/K).

Sedimentation Velocity Analytical Ultracentrifugation. Sedimentation velocity experiments were performed at 20 °C using an Optima XL-A analytical ultracentrifuge (AUC) (Beckman Coulter, Fullerton, CA) equipped with an absorbance detection system and a four-hole AN-60 Ti rotor. The rotor was pre-chilled and equilibrated for an hour prior to the start of the run. All experiments were carried out at a radial step size of 0.003 cm in continuous mode and with no delay between each scan.

Prior to centrifugation, SsuE and MsuE were buffer exchanged into 25 mM phosphate buffer (pH 7.5) and 100 mM NaCl using an Amicon Ultra—4 centrifugal filter with a molecular weight cutoff of 10 kDa from Millipore (Burlington, MA). The AUC experiments were carried out at different rotor speeds based on the mass of the reductases and substrate. SsuE (12 μM) and MsuE (20 μM) were utilized for the initial determination of the sedimentation coefficients in the absence and presence of flavin. Standard epon-double sector centerpieces of 12 mm were loaded with sample in the sample cell and 25 mM phosphate buffer (pH 7.5) and 100 mM NaCl in the reference cell. For experiments performed in the presence of FMN, flavin concentrations at five times the concentrations of the reductases (SsuE and MsuE) were added to 1 mL of the enzymes. The samples were washed three times with 4.0 mL of 25 mM potassium phosphate (pH 7.5) and 100 mM NaCl. Unbound flavin was removed from the samples by centrifugation at 5000 rpm for 10 min, utilizing the centrifugal filter so that the free flavin would not contribute to the 280 nm absorbance. The concentrations of SsuE (12 μM) and MsuE (20 μM) were determined using the flavin absorbance at 450 nm (12.2 mM^{-1} cm^{-1}). Radial absorbance scans at 280 nm were collected continuously at 37,000 and 40,000 rpm for SsuE and SsuE/FMN and 40,000 and 37,000 rpm for MsuE and MsuE/FMN, respectively.

Data derived from the scans were evaluated using the continuous sedimentation distribution model $c(s)$ with the SEDFIT program using the numerical Lamm equation. Sednterp was used to calculate the fitting parameters for SEDFIT.[22] The partial specific volume of 0.7440 cm^3/g for SsuE and 0.7552 cm^3/g for MsuE was calculated based on their amino acid composition at 20 °C. A buffer density of 1.00574 g/mL and a viscosity of 1.0183 cP were calculated based on the buffer composition of 25 mM phosphate using the same program. A frictional coefficient (f/f_0) of 1.3 for both SsuE and MsuE was used to fit the sedimentation velocity scans.

Differential H/D-X Experiments. *H/D-X MS Experiments.* Local amide H/D exchange experiments were carried out using a fully automated system (PAL, LEAP Technologies, Carrboro, NC). Prior to differential H/D-exchange analysis, SsuE and MsuE apoenzymes were buffer exchanged (25 mM phosphate buffer, pH 7.5, 100 μM NaCl) using an Amicon Ultra-4 centrifugal filter (10 kDa MWCO, Millipore). H/D-exchange reactions for SsuE and MsuE (20 μM) apoenzymes were initiated by mixing with a 20-fold (v/v) excess of D_2O-containing exchange buffer (57 μL, phosphate buffer, 25 mM, pD 7.5, 100 μM NaCl). After incubation for 10, 60, 300, 600, 900, or 1800 s at 20 °C for SsuE or 10, 60, 300, 600, and 900 s for MsuE, unwanted back exchange was minimized with the addition of 1 equiv (v/v, 60 μL) of cold quench solution (200 mM phosphate buffer, pH 2.5, 0 °C). For unlabeled reactions (e.g., "0 s exchange"), apoenzymes were mixed with a 20-fold excess of H_2O-containing buffer (phosphate buffer, 25 mM, pH 7.5, 100 mM NaCl) and quenched as above.

Differential H/D-exchange for substrate bound proteins were measured using freshly buffer-exchanged SsuE and MsuE (20 μM). Proteins were incubated on ice with a 5-fold molar excess of either FMN (100 μM) or NADPH (100 μM) for

https://doi.org/10.1021/acs.biochem.3c00361
Biochemistry 2023, 62, 2751−2762

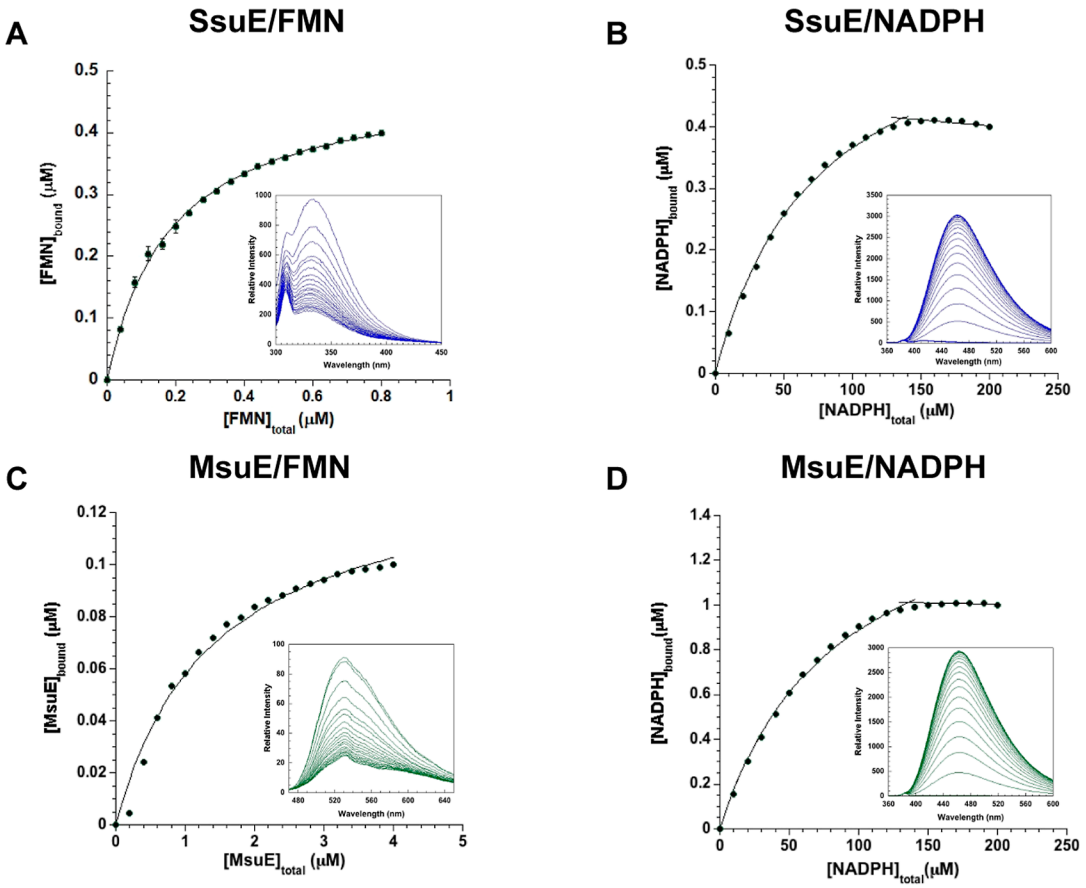

Figure 1. Fluorescent titrations of SsuE and MsuE with FMN and NADPH. (A) Titration of SsuE (0.04 μM) with FMN (0.04−0.4; λ_{ex}, 280 nm; and λ_{em}, 342 nm). (B) Titration of SsuE (0.04 μM) with NADH (10−200 μM; λ_{ex}, 340 nm; and λ_{em}, 450 nm). (C) Titration of FMN (0.1 μM) with MsuE (0.2−4.0 μM; λ_{ex}, 450 nm; and λ_{em}, 525 nm). (D) Titration of MsuE (1 μM) with NADPH (10−200 μM; λ_{ex}, 340 nm; and λ_{em}, 450 nm). All titration experiments were performed in triplicate and fit to a quadratic equation for single-site binding.

~20 min prior to analysis. Exchange reactions were monitored at 0, 10, 60, 300, 600, 900, or 1800 s for SsuE and 0, 10, 60, 300, 600, 900 s for MsuE at 20 °C, quenched with quench solution, and digested as above. After quenching, samples (100 μL) were immediately loaded onto an Enzymate BEH Pepsin Column (2.1 × 30 mm, 5 μm). Digestion temperature was maintained at 12 °C, a flow rate of 250 μL/min, and a pressure of ~8000 psi for 4 min. Peptides (10−15 pmol) were subjected to LC/MS−MS analysis immediately following digestion. To help prevent sample carry-over, the inline pepsin column was washed (1.5 M GuHCl, 4% acetonitrile, 0.8% formic acid, pH 2.5) after each digestion, and clean blank injections (0.1% formic acid) were run after every protein injection. H/D exchange reactions were performed in duplicate.

LC/MS−MS. LC−MS/MS analysis was performed using a Synapt XS ion-mobility-assisted mass spectrometer in positive mode (Waters, Manchester, UK) coupled to a nano-Acquity UPLC/H/D-X manager system (Waters, Manchester, UK). Post-pepsin-digested products were directly loaded onto an Acquity UPLC BEH C18 Vanguard trapping column (1 × 5 mm, 250 μL/min) and desalted for 4 min. Peptides were separated on an Acquity UPLC BEH C18 1.7 μm analytical column (1 × 50 mm) using an effective 8 min linear gradient starting at 5% acetonitrile, 0.1% formic acid, and increasing over 7 min to 60% acetonitrile and 0.1% formic acid with a flow rate of 150 μL/min. All chromatographic steps, including trapping and elution, were performed at 2 °C. Ion mobility assisted HD MS^E data were collected with an ESI capillary voltage of 32 V and the quadrupole used in rf-mode; only ions with m/z > 300 were transmitted. For ion mobility, the T-wave was operated with a wave height of 40 V and a wave velocity ramp from 500 to 800 m/s; collision energy in the trap was continuously alternated between low energy (4 V) and high energy (20−35 V) throughout the run. For all measurements, ToF was acquired in resolution mode with a scan time of 0.4 s. Data were lock-mass corrected post-acquisition using the +1 charge state of LeuEnk [MH^+ 556.2771], which was infused at a concentration of 200 pg/μL at 90° to the analytical sprayer at 10 μL/min throughout the acquisition.

Peptide Identification and Data Processing. Data were processed using ProteinLynx Global Server (PLGS v 3.03). Data were centroided, de-isotoped, and the charge state was reduced prior to fragment ion and parent protein assignments based on retention time alignments. Peak picking thresholds were optimized using the PLGS Threshold Inspector: 25 counts and 100 counts were used for all high and low energies. Peak lists were searched against databases containing either *E. coli* SsuE (Uniprot P80644) or *Pseudomonas aeruginosa* MsuE (Uniprot ID O31038) and porcine pepsin (Uniprot P00791). Protein identification criteria were set as the detection of at least 3 fragments per protein, 3 fragments per peptide, and 1 peptide per protein. Methionine oxidation was set as a variable modification for all searches. The protein level false discovery

https://doi.org/10.1021/acs.biochem.3c00361
Biochemistry 2023, 62, 2751−2762

rate was set to 4%. PLGS search results and deuterium exchange spectra were imported into DynamX (v 3.0), and peptides were filtered based on the following criteria: 3 fragments per peptide, 2 fragments must be adjacent, have a minimum of 0.1−0.2 products per amino acid residue, and be present in all of the LC/MS−MS injections. Deuterium exchange measurements were analyzed with default settings, and the data were manually inspected, validated, and curated. In keeping with newly recommended reporting standards for H/DX MS experiments, peptide coverage maps, uptake plots (Figures S3−S8), and H/D-exchange summary data files (File S2) are provided. For all datasets, differences in fractional deuterium uptake over time or between conditions were mapped onto SsuE (PDB: 4PU0) and an AlphaFold model of the MsuE dimer and tetramer using scripts generated in DynamX and PyMOL.[23,24]

RESULTS

Substrate Affinity and Stability. The binding affinities of the alkanesulfonate FMN reductase enzymes were evaluated to compare the substrate specificity between SsuE and MsuE. Intrinsic Trp fluorescence was utilized to monitor flavin binding to SsuE. Given the lack of Trp residues in MsuE, titrations were performed, monitoring the decrease in flavin fluorescence. SsuE showed a clear flavin preference with an ∼40-fold lower K_d value for FMN than FAD (Figure 1A, Table 1, and Figure S1A), but the enzyme showed a similar affinity for NADPH and NADH (Figure 1B, Table 1, and Figure S1B). The fluorescence decrease observed at higher pyridine nucleotide concentrations is due to unbound NADPH in solution.[25] MsuE and the MsuD monooxygenase partner had a distinct specificity for FMN and NADPH in coupled assays with the MsuD monooxygenase partner, but the specificity of MsuE for each substrate in the absence of MsuD had not been determined.[21] MsuE showed a similar affinity for FMN/FAD and NADH/NADPH, indicating there was no apparent preference for a specific substrate under equilibrium conditions (Figure 1C,D, Table 1, and Figure S1C,D).

Table 1. Substrate Binding Affinity of SsuE and MsuE

	K_{FMN} (μM)	K_{FAD} (μM)	K_{NADPH} (μM)	K_{NADH} (μM)
SsuE	0.26 ± 0.03	11 ± 1	75 ± 5	55 ± 5
MsuE	1.4 ± 0.1	0.8 ± 0.2	84 ± 5	51 ± 3

Oligomeric State of SsuE and MsuE. Alternative oligomeric forms for SsuE have been reported based on the experimental procedure used for analysis. We had previously observed an apparent oligomeric shift from a tetramer to a dimer for SsuE when FMN was included in the sample, but comparable studies have not been performed with NADPH.[4,10] In addition, there have been no studies to evaluate the oligomeric state of MsuE in the apo form or with the addition of substrates. Molecular weight species of SsuE and MsuE were evaluated by native-PAGE in the apo form and with the addition of substrates. The majority of the apo SsuE protein ran as a higher molecular weight band compared to the SsuE/FMN complex (Figure 2A). This shift in molecular weight for the SsuE/FMN complex could correlate with an alternative conformer. A similar gel shift was not observed with SsuE and NADPH (Figure 2B). Both the apo MsuE and MsuE/FMN complexes separated at a similar molecular weight, suggesting the MsuE/FMN complex did not cause an alteration in the molecular weight as was observed for SsuE (Figure 2A). Similar to SsuE, MsuE with the NADPH substrate did not show a band shift for the separated enzyme (Figure 2B).

The band shift observed for SsuE on Native-PAGE suggests a structural change may have occurred with the addition of FMN. However, a detailed analysis of which factors trigger these changes in solution has not been performed. AUC was performed to identify the oligomeric state(s) of apo SsuE and MsuE in solution. SsuE in the absence of substrate gave a sedimentation value ($s20,w$) of 4.55 ± 0.10 S, which corresponded to a molecular mass of 81.5 ± 4.6 kDa (Figure 3A and Table 2). With a monomeric molecular mass of 21.3 kD for SsuE, the protein existed predominately as a tetramer in the apo form. Given the structural similarity between SsuE and MsuE, we expected that MsuE would also exist as a tetramer, but AUC analyses of MsuE gave an $s20,w$ value of 4.14 ± 0.13 S, corresponding to a molecular weight of 42.4 ± 1.2 kDa consistent with a dimer (MsuE monomeric molecular weight, ∼20.0 kDa) (Figure 3B and Table 2). Interestingly, for the SsuE/FMN sample, there were two species observed ($s20,w$; 4.51 ± 0.04 and 3.31 ± 0.13 S) corresponding to a tetramer (78.3 ± 1.3 kDa) and dimer (49.3 ± 3.3 kDa) (Figure 3A and Table 2). Therefore, the SsuE/FMN complex shifted the quaternary structure of the enzyme from a tetramer to a tetramer/dimer equilibrium. Although the dimer was not identified from a fit of the sedimentation profiles of apo SsuE, there was some tailing on the left side of the sedimentation distribution plot, indicating there may be a small amount of dimer in the absence of substrates. Contrary to the findings for the SsuE/FMN complex, the addition of FMN to MsuE resulted in a single higher molecular weight species (80.7 ± 0.9 kDa) that corresponded to a tetramer (Figure 3B and Table 2). Changes to the oligomeric state of SsuE and MsuE were also

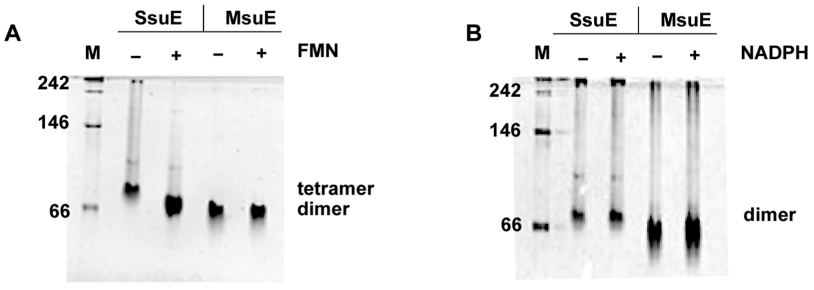

Figure 2. Native-PAGE analyses of SsuE and MsuE. (A) Separation of apo SsuE or MsuE and the SsuE or MsuE/FMN complex. (B) Separation of apo SsuE or MsuE and the SsuE or MsuE/NADPH complex. M: native gel molecular weight markers. Proteins were separated on 12% native PAGE.

https://doi.org/10.1021/acs.biochem.3c00361
Biochemistry 2023, 62, 2751−2762

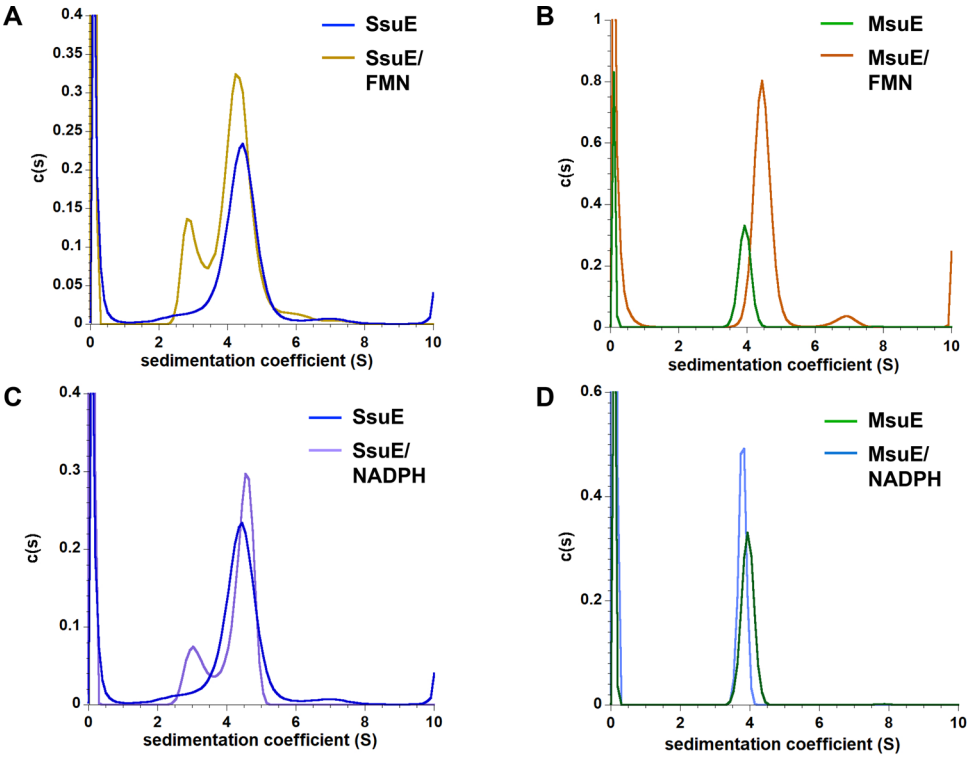

Figure 3. Sedimentation distribution plots of SsuE and MsuE. (A) SsuE and SsuE/FMN, (B) MsuE and MsuE/FMN, (C) SsuE and SsuE/NADPH, and (D) MsuE and MsuE/NADPH. AUC experiments were performed with SsuE (12 μM) and MsuE (20 μM). FMN and NADPH were added 5-fold over the enzyme concentration for both SsuE and MsuE. The reactions were performed in triplicate, but only one fit from each analysis is shown for clarity.

Table 2. Results from AUC Analysis of SsuE and MsuE

	SsuE (kDa)	SsuE + FMN (kDa)		SsuE + NADPH (kDa)	
*s*20,*w* (S)	4.55 ± 0.10	4.51 ± 0.04	3.31 ± 0.13	4.70 ± 0.05	3.15 ± 0.15
molecular weight (kDa)	81.5 ± 4.6	78.3 ± 1.3	49.3 ± 3.3	79.3 ± 2.4	43.8 ± 4.1
	MsuE (kDa)	MsuE + FMN (kDa)		MsuE + NADPH (kDa)	
*s*20,*w* (S)	4.14 ± 0.13	4.60 ± 0.02		3.96 ± 0.03	
molecular weight (kDa)	42.4 ± 0.3	80.7 ± 0.9		48.5 ± 0.4	

evaluated with the addition of NADPH. While the dimer was less pronounced, a similar tetramer to dimer equilibrium shift was also observed with the SsuE/NADPH complex (Figure 3C and Table 2). However, MsuE with NADPH was predominately in the dimeric form and did not shift to a tetramer like the MsuE/FMN complex (Figure 3B,D and Table 2).

Thermal Stability of SsuE and MsuE. AUC studies demonstrated alterations in the oligomeric state of SsuE and MsuE under specific conditions for each enzyme. Therefore, the binding of substrates and subsequent oligomeric changes may alter the stability of the proteins. The thermal melting temperatures of SsuE and MsuE were evaluated by thermal melt CD spectroscopy to determine if alterations in the oligomeric states affected the structural stability of the enzymes. The T_m value of apo SsuE was 47.5 ± 0.2 °C using a temperature range from 20 to 94 °C (Figure 4A and Table 3). Although apo MsuE existed as a dimer, the enzyme had a similar melting temperature in the absence of substrates as SsuE (Figure 4B and Table 3). Interestingly, the T_m value increased for both SsuE and MsuE when FMN was included (Figure 4C,D and Table 3). For SsuE, the change from a tetramer to a dimer/tetramer equilibrium with the addition of FMN led to a sharp increase in the melting temperature (75.2 ± 0.1 °C) compared to apo SsuE (Figure 4C and Table 3). However, a similar increase in melting temperature was not observed with NADPH (Figure S2A). The oligomeric change of MsuE from a dimer to a tetramer in the presence of FMN also resulted in an increase in the melting temperature (60.8 ± 0.2 °C) that was not observed with NADPH (Figure 4D, Figure S2B). The change in melting temperature with the addition of FMN suggested that the conformational alteration in the oligomeric state of each enzyme increased enzyme stability. It was curious that even though SsuE and MsuE have different oligomeric states in the presence of FMN, they showed similar increases in the melting temperature and increased stability. For SsuE/FMN, the CD spectra for the enzyme complex at 90 °C showed a difference in absorbance between 220 and 240 nm that was not observed in SsuE only. The apo SsuE enzyme still showed some secondary structural features indicative of a random coil compared to the SsuE/FMN complex, which showed no secondary structural features.

H/D-Exchange Mass Spectrometry. H/D-exchange (H/D-X) mass spectrometry (MS) experiments were performed to further probe the solution dynamics of the SsuE and MsuE dimer/tetramer equilibrium in the absence or presence of FMN and NADPH. H/D-X measures the propensity of main-

https://doi.org/10.1021/acs.biochem.3c00361
Biochemistry 2023, 62, 2751−2762

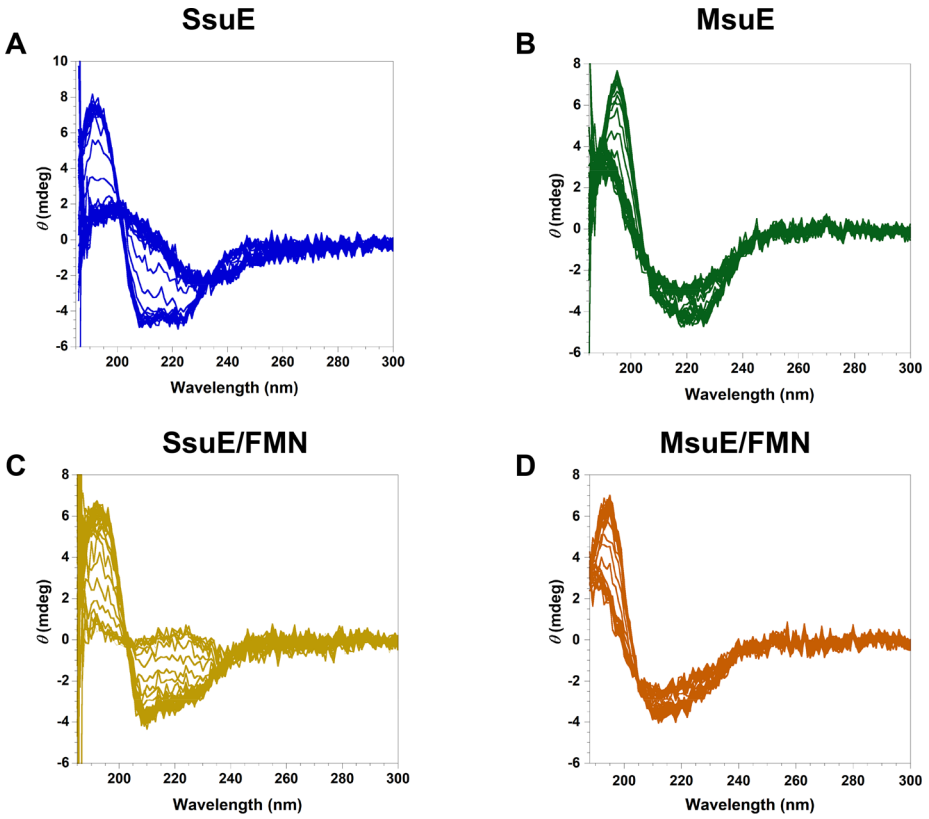

Figure 4. Thermal denaturation CD of SsuE and MsuE. (A) SsuE, (B) MsuE, (C) SsuE/FMN, and (D) MsuE/FMN. SsuE and MsuE (5 μM) were scanned over a wavelength range of 185−300 nm and a temperature range of 20−94 °C. FMN was added in a 1:10 ratio (enzyme: substrate) when included. Each thermal denaturation experiment was performed in triplicate.

Table 3. Thermal Stability of SsuE and MsuE

	T_m		
	(°C)	+FMN (°C)	+NADPH (°C)
SsuE	47.5 ± 0.2	75.2 ± 0.1	46 ± 1
MsuE	48.5 ± 0.2	60.8 ± 0.2	46 ± 1

chain amide protons to exchange with the bulk solvent. Protons that are solvent-inaccessible or contained within a strong hydrogen-bonding network will not undergo exchange as readily as those that are exposed to solvent and not extensively involved in hydrogen bonding interactions.[26] Because amide protons in dimer/dimer interfaces are often protected in H/D-X studies, these experiments afford us the means to compare the ligand-stabilized, higher-order structural rearrangement mechanisms of SsuE and MsuE.[27,28] SsuE and MsuE are both highly amenable to interrogation by H/D-X MS. For example, 100% coverage was obtained for SsuE (average peptide lengths of ∼13 residues, redundancy of ∼3.5−4) in the absence or presence of FMN or NADPH (Figure S3). Due to the instability of SsuE, exchange reactions were only monitored to 30 min; however, this was ample time to examine the impact of FMN and NADPH on the dimer/tetramer equilibrium. Upon initial inspection, differential H/D-X between SsuE/FMN and apo SsuE indicated FMN reduces deuterium uptake, even at a 10 s exposure time (Figure 5A). Longer exposure times showed greater differences between SsuE/FMN and apo SsuE (Figure 5B,C), which was especially apparent at the dimer/dimer interface (Figure 5D). Considering the apo SsuE apoenzyme is proposed to exist as a tetramer and the SsuE/FMN complex establishes a dimer/tetramer equilibrium, we expected to see more uptake in the presence of FMN compared to the apoenzyme as the residues contained within the dimer/dimer interface should be more exposed. Inspection of the isotopic distributions in the mass spectra revealed bimodal distribution patterns for the apoenzyme and SsuE/FMN (Figure 5E and Table S1). Bimodal distribution patterns are commonly observed when there is significant heterogeneity in the higher-order structures.[29,30] The SsuE/FMN complex adopts two different higher-ordered structures in the sample, one of which protects against deuterium uptake more than the other. The bimodal distributions observed for apo SsuE and SsuE/FMN are most likely due to the presence of dimers (fast-exchanging) and tetramers (slow-exchanging). The bimodal exchange patterns were largely observed in regions of SsuE near the dimer/dimer interface and around the π-helix (residues 22−48, 71−84, and 90−138; Table 1). There was little variation in the overall amount of deuterium exchanged over time in the uptake plots of apo SsuE (Figure S4). The observed bimodal distributions were likely due to the rapid exchange (<10 s) of solvent for the dimer population at the dimer/dimer interface. In contrast, isotopic distributions of SsuE in the presence of FMN showed both binomial and bimodal exchange patterns at early timepoints, with the tetramer being the predominant species. Longer exposure times consistently showed the appearance of the fast-exchanging dimer, with nearly equal distribution between the dimer and tetramer. While similar bimodal patterns of exchange were observed in the presence of NADPH, the distributions of dimer and tetramer species were consistent with those observed for the apoenzyme, giving rise to nearly identical uptake plots (Figure S5).

https://doi.org/10.1021/acs.biochem.3c00361
Biochemistry 2023, 62, 2751−2762

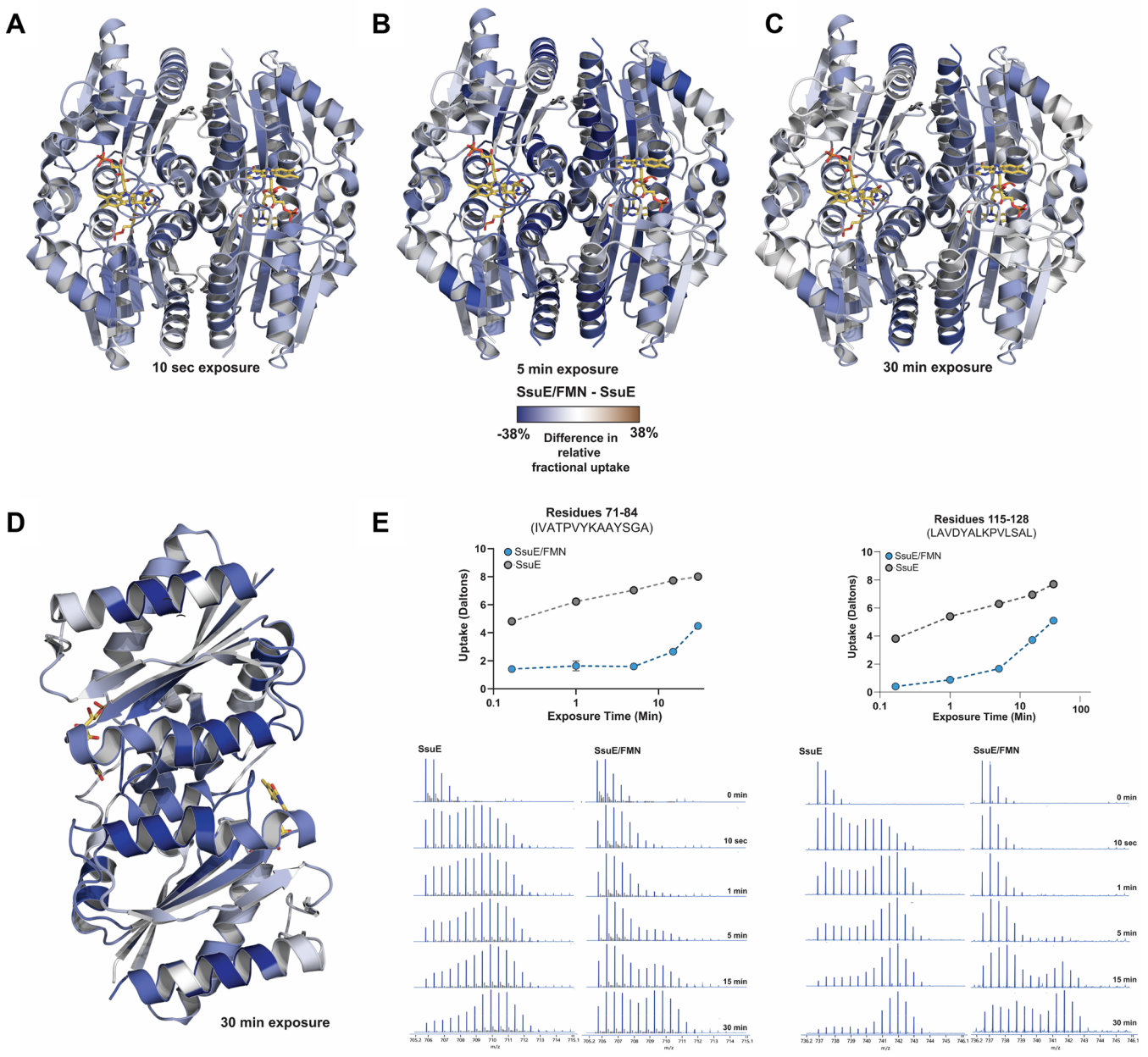

Figure 5. Differential H/D-X analysis of SsuE and SsuE/FMN. Differences in relative fractional uptake after (A) 10 s, (B) 5 min, and (C) 30 min of D_2O exposure for SsuE/FMN and SsuE mapped onto the SsuE tetramer. Protein regions showing decreased deuterium in the presence of FMN are shown in blue, regions with no difference in exchange are shown in white, and regions where FMN increases deuterium uptake compared to the apoenzyme are shown in brown. (D) Differential H/D-X mapped onto the SsuE dimer for 30 min of D_2O exposure. Colors as defined in (A−C). To highlight the dimer/dimer interface, the dimer of (C) is rotated 180°. (E) Representative deuterium uptake plots and peptide spectra showing bimodal distributions of the isotopic envelope, indicating a mixed population of dimer (fast exchanging, higher m/z) and tetramer (slower exchanging, lower m/z) species. Exchange patterns for all peptides identified are summarized in Table S2 and all deuterium uptake plots for SsuE/FMN and SsuE/NADPH are provided in Figures S4 and S5.

Like SsuE, MsuE is equally amenable to interrogation by H/D-X. Peptide coverage was obtained for nearly the entire protein (98.6−99%) with high redundancy (Figure S6). Unlike SsuE, the MsuE apoenzyme and MsuE/FMN complex displayed binomial isotopic distributions in the mass spectra, suggesting a more homogeneous mixture of higher-order structures (HD/X Summary and Data Files). Differential H/D-X analysis of MsuE/FMN compared to MsuE showed a marked decrease in deuterium uptake in the presence of FMN (Figure 6A), which was most apparent at the dimer/dimer interface (Figure 6B) and in regions proposed to stabilize the interface (Figure 6C). As seen in the uptake plots (Figure S7), the decreased deuterium uptake in the presence of FMN was largely due to changes in solvent exposure, or overall deuterium uptake, rather than changes in protein motions or dynamics. Collectively, these data suggest FMN stabilizes MsuE in a single, tetrameric species. In striking contrast, MsuE/NADPH shows no significant difference in deuterium uptake compared to the exchange observed for the apoenzyme. Deuterium uptake plots (Figure S8) for all peptides analyzed are nearly identical in both exchange rates and relative

https://doi.org/10.1021/acs.biochem.3c00361
Biochemistry 2023, 62, 2751−2762

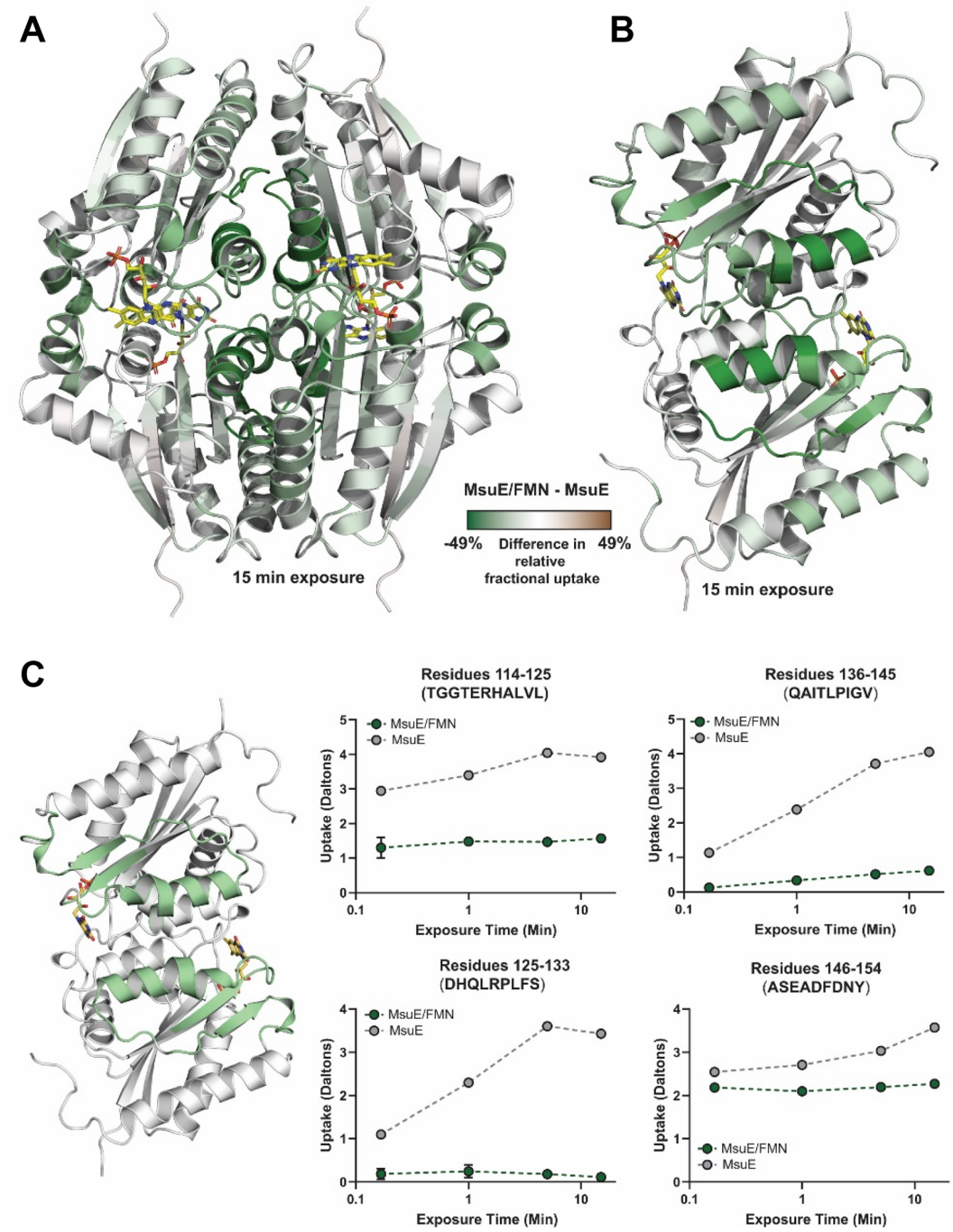

Figure 6. Differential H/D-X analysis of MsuE and MsuE/FMN. Differences in relative fractional uptake after 15 min of D_2O exposure for MsuE/FMN and MsuE mapped onto the MsuE tetramer (A) and dimer (B). Protein regions showing decreased deuterium in the presence of FMN are shown in green, regions with no difference in exchange are shown in white, and regions where FMN increases deuterium uptake compared to the apoenzyme are shown in brown. To highlight the dimer/dimer interface, the dimer of (A) is rotated 180°. (C) Deuterium uptake plots for the dimer/dimer interface, including the π-helix. Protein residues captured in these select uptake plots are highlighted on the MsuE/FMN dimer structure (pale green). Deuterium uptake plots for MsuE/FMN and MsuE/NADPH are provided in Figures S7 and S8.

deuterium incorporation, indicating NADPH has little impact on the dimer/tetramer equilibrium of MsuE.

DISCUSSION

Protein oligomers have evolved because of their advantage over monomeric states. These advantages include the possibility of allosteric control, higher local concentrations of active sites, larger binding surfaces, new active sites at subunit interfaces, and economic ways to produce large protein interaction networks and molecular machines.[31−33] Oligomeric changes have been identified for specific FMN-dependent reductases associated with two-component monooxygenase systems.[10,15,34,35] Factors that initiate these observed oligomeric changes include interactions with the monooxygenase enzyme, fluctuations in cellular concentrations of the enzyme, and substrate binding. The SsuE and MsuE FMN-reductases are part of two-component enzyme systems involved in sulfur acquisition. While SsuE has a single monooxygenase partner,

https://doi.org/10.1021/acs.biochem.3c00361
Biochemistry 2023, 62, 2751−2762

MsuE must be able to transfer flavin to two structurally and functionally different monooxygenase enzymes.[8,9,36] SsuE and MsuE are classified in the group of NADPH/FMN reductases that are part of the flavodoxin-like superfamily based on their structural similarities.[10] Members of this group include NADPH/FMN reductases with a tightly bound FMN prosthetic group and enzymes that use FMN as a substrate such as SsuE and MsuE. The principal structural difference between the two groups of enzymes is the presence of a π-helix located at the dimer/dimer interface.[10,21,37,38] It has been proposed that the π-helix structure enables SsuE to transfer flavin through protein−protein interactions to the SsuD monooxygenase partner.[11−13,39] The SsuE−SsuD interaction sites are located at the dimer/dimer interface of SsuE so the enzyme would need to undergo a conformational change to form these interactions.[4,10,37,38] Comparable protein−protein interactions between MsuE and the MsuC/MsuD monooxygenases have not been evaluated. A substrate-induced oligomeric change precipitated by the π-helix would be a viable mechanism to promote protein−protein interactions and ready the enzymes for flavin transfer.

The FMN reductases and monooxygenases from two-component systems have a preference for a specific redox form of the flavin. The FMN reductases typically show a higher affinity for oxidized flavin and their partner monooxygenases prefer reduced flavin.[40,41] This specificity ensures that the reduced flavin is transferred to the monooxygenase enzyme. Detailed substrate binding analyses of SsuE and MsuE were performed in order to identify the preferred substrate for each enzyme to use in further studies to evaluate oligomeric state changes in the presence of each substrate. SsuE showed a preference for FMN but was able to use either NADH or NADPH for flavin reduction. The MsuE enzyme showed a similar affinity for FMN/FAD and for each pyridine nucleotide. Although MsuE showed no clear preference for a specific pyridine nucleotide in binding studies, FMN and NADPH are the preferred substrates in coupled assays with the monooxygenase enzyme MsuD monitoring desulfonation. Similar to other FMN reductases, the mechanism of flavin reduction by SsuE was previously shown to utilize a sequential mechanism for binding with the pyridine nucleotide binding first followed by the flavin to form a ternary complex.[20] Following flavin reduction, the reduced flavin is transferred to the monooxygenase and the pyridine nucleotide is released. The preference for NADPH in coupled assays with MsuE/MsuD could be related to the release of the oxidized pyridine product to promote continued flavin reduction by MsuE if a similar binding model as SsuE is used. Moreover, MsuD must be altering the preference of MsuE for NADPH as the specificity is only observed in coupled assays.

The established substrate preference was used to determine if oligomeric changes were initiated by specific substrate binding. Given the structural and functional similarity of MsuE and SsuE with the comparable π-helix providing a gain of function, we anticipated that similar oligomeric changes would be observed between the two enzymes. SsuE existed in different multimeric states in the presence of FMN and NADPH compared to the apo enzyme. With the addition of FMN or NADPH, SsuE shifted from a tetramer to a tetramer/dimer equilibrium. The rapid shift between tetramer and dimer species would lead to the exposed regions of the dimer exchanging over longer exposure times in H/D-X MS studies, even though the tetramer was the predominant species in solution. This would give inflated deuterium uptake measurements for the apoenzyme at longer (>5 min) time points. In contrast, FMN slows the rapid equilibrium between the dimer and tetramer, which is evident from the slow appearance of the dimer in the mass spectra. The shift from the tetramer to a dimer occurred along the dimer/dimer interface of SsuE. An oligomeric shift would disrupt the hydrogen bonding interactions between the insertional tyrosine residue of the π-helices and the amide of the peptide backbone across the dimer/dimer interface. The presence of π-helices in proteins often leads to increased flexibility due to the altered intrastrand hydrogen bonding. For soybean lipoxygenase, the π-helix becomes mobile on a nanosecond timescale with the binding of lipid.[42] The substrate binding sites of SsuE are located near the π-helices and the binding of flavin may lead to an initial increase in mobility, resulting in the disruption of hydrogen bonding interactions across the dimer/dimer interface. Although SsuE with flavin bound exists as a tetramer in the three-dimensional structure, the preformed crystals of SsuE were soaked with FMN so the tetramer observed may not be an accurate representation of oligomeric states for SsuE.[10]

For MsuE, the enzyme shifted from a dimer to a tetramer with the addition of flavin, but there was no change in the oligomeric state with NADPH. The shift to a tetramer was also supported by H/D-X MS studies that demonstrated decreased deuterium uptake at the dimer/dimer interface for the MsuE/FMN complex compared to the apo enzyme. The decreased deuterium uptake for the MsuE/FMN complex was primarily located in the π-helical region. Therefore, the π-helices form the core of the MsuE tetramer, similar to SsuE. Based on these investigations, apo MsuE exists as a dimer, and the addition of FMN converts the enzyme to a tetramer with the π-helices located at the dimer/dimer interface.

The changes in the oligomeric state for both SsuE and MsuE with FMN bound likely represent a regulatory control point for reduced flavin transfer. The differences in the observed oligomeric states between SsuE and MsuE were surprising given their structural similarity and are likely a result of their different physiological roles. Despite these differences, both SsuE and MsuE demonstrated a pronounced increase in enzyme thermal stability with the FMN substrate. It is not overtly apparent why there was an observed increase in the T_m of the enzyme with FMN bound. There are no major structural changes between the monomeric three-dimensional structure of apo SsuE and the SsuE/FMN complex. However, a decrease in H/D exchange was observed in the β-sheets located at the center of SsuE at all time points, indicating a more compact or rigid structure that would be more resistant to thermal denaturation. An increase in stability would also assist in stabilizing the flavin prior to the reduction. The dimer/dimer interface of SsuE forms protein−protein interactions with SsuD, and the tetrameric form of SsuE would have to dissociate along the dimer/dimer interface to interact with SsuD (Figure 7A). Therefore, the conversion of SsuE to a tetramer/dimer equilibrium in the presence of substrates would promote these interactions. Binding of dimeric SsuE to SsuD would lead to a tetramer/dimer equilibrium shift to promote protein−protein interactions. Conversely, MsuE shifted from a dimer to a tetramer with the binding of FMN only, and multiple oligomeric states were not observed (Figure 7B). The additional noncovalent interactions to form the tetramer and bind FMN could lead to the observed increase in thermal stability with the MsuE/FMN complex. Based on the

https://doi.org/10.1021/acs.biochem.3c00361
Biochemistry 2023, 62, 2751−2762

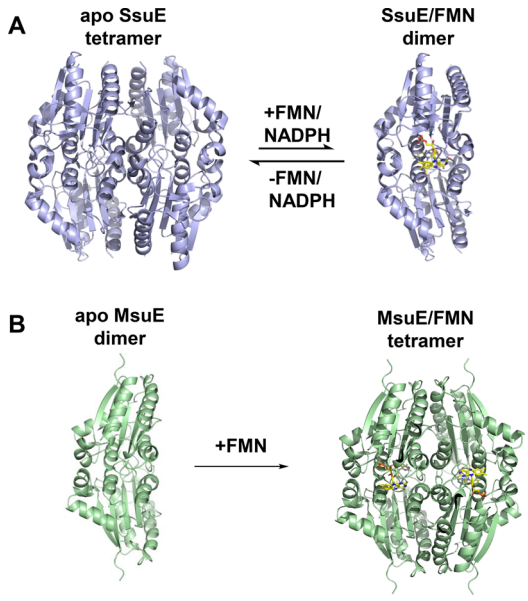

Figure 7. Model for SsuE and MsuE oligomeric changes. (A) SsuE shifts from a tetramer to a slow tetramer/dimer equilibrium with the addition of FMN or NADPH. (B) MsuE shifts from a dimer to a tetramer with the addition of FMN. Oligomeric change was not observed with NADPH. PDB: 4PU0 (SsuE), MsuE was generated with AlphaFold.[10,23]

location of the flavin at the dimer/dimer interface in structural models, it would be difficult to release the flavin unless MsuE was in the dimeric form. MsuE was shown to play a dual role in providing reduced flavin FMN to both MsuC and MsuD.[8,9] If MsuE forms protein−protein interactions with both MsuC and MsuD, then these interactions and/or FMN reduction may be the catalyst that drives the equilibrium shift from a tetramer to a dimer. Alternatively, flavin transfer in MsuE may occur by a diffusion mechanism and no protein−protein interactions would be necessary. However, it would be difficult to transfer reduced flavin in the tetrameric species of MsuE as the substrate is buried at the dimer/dimer interface. Current studies to evaluate the oligomeric state of SsuE and MsuE in the presence of their partner monooxygenases will provide additional insight into the observed oligomeric changes between the apo and FMN-bound enzyme. Although SsuE and MsuE share ∼30% amino acid sequence identity, there is a clear difference in the oligomeric changes that is likely related to differences in their overall functional role.

■ ASSOCIATED CONTENT

Supporting Information

The Supporting Information is available free of charge at https://pubs.acs.org/doi/10.1021/acs.biochem.3c00361.

Fluorescent titrations and thermal denaturation CD of SsuE and MsuE; coverage map for SsuE; uptake plots for differential H/D-X analysis; and H/D-X patterns for SsuE peptides determined for the apoenzyme (PDF)

H/D-X summary and data files (XLSX)

Accession Codes

SsuE (UniProt entry: P80644) and MsuE (UniProt entry: Q88J85).

■ AUTHOR INFORMATION

Corresponding Author

Holly R. Ellis − *Department of Biochemistry and Molecular Biology, Brody School of Medicine at East Carolina University, Greenville, North Carolina 27834, United States;* orcid.org/0000-0003-0521-422X; Email: ellish20@ecu.edu

Authors

Chioma H. Aloh − *Department of Biochemistry and Molecular Biology, Brody School of Medicine at East Carolina University, Greenville, North Carolina 27834, United States*

Tonya N. Zeczycki − *Department of Biochemistry and Molecular Biology, Brody School of Medicine at East Carolina University, Greenville, North Carolina 27834, United States;* orcid.org/0000-0002-5216-1960

Complete contact information is available at: https://pubs.acs.org/10.1021/acs.biochem.3c00361

Author Contributions

The manuscript was written by C.H.A. and edited and revised by H.R.E. and T.N.Z. Different aspects of the experimental plan were conceptualized by the authors. Except for H/D-X MS, C.H.A. performed all the experiments and analyzed the data. C.H.A. provided protein for H/D-X MS, and the data for H/D-X MS was collected at the Brody School of Medicine Mass Spectrometry Core at ECU by the Core Director, T.N.Z. The H/D-X MS data was analyzed by H.R.E. and T.N.Z. All authors have approved the final version of the manuscript.

Notes

The authors declare no competing financial interest.

■ ACKNOWLEDGMENTS

This work was supported by NSF grant 2105998 (H.R.E.) and the Brody School of Medicine Mass Spectrometry Core at ECU, which has received support from the Golden Leaf Foundation and from federal COVID-19 relief funds appropriated to ECU in North Carolina SL 2020-4.

■ ABBREVIATIONS

AUC, analytical ultracentrifugation; CD, circular dichroism; H/D-X MS, hydrogen deuterium exchange mass spectrometry; MsuC, methanesulfinate monooxygenase; MsuD, methanesulfonate monooxygenase; MsuE, methanesulfinate/methanesulfonate monooxygenase FMN reductase; SsuD, alkanesulfonate monooxygenase; SsuE, alkanesulfonate monooxygenase FMN-dependent reductase

■ REFERENCES

(1) Kertesz, M. A.; Leisinger, T.; Cook, A. M. Proteins induced by sulfate limitation in Escherichia coli, Pseudomonas putida, or Staphylococcus aureus. *J. Bacteriol.* **1993**, *175*, 1187−1190.

(2) Kertesz, M.; Wietek, C. Desulfurization and desulfonation: applications of sulfur-controlled gene expression in bacteria. *Appl. Microbiol. Biotechnol.* **2001**, *57*, 460−466.

(3) Kertesz, M. A. Riding the sulfur cycle–metabolism of sulfonates and sulfate esters in gram-negative bacteria. *FEMS Microbiol. Rev.* **2000**, *24*, 135−175.

(4) Eichhorn, E.; van der Ploeg, J. R.; Leisinger, T. Characterization of a two-component alkanesulfonate monooxygenase from Escherichia coli. *J. Biol. Chem.* **1999**, *274*, 26639−26646.

(5) van Der Ploeg, J. R.; Iwanicka-Nowicka, R.; Bykowski, T.; Hryniewicz, M. M.; Leisinger, T. The *Escherichia coli ssuEADCB* gene cluster is required for the utilization of sulfur from aliphatic sulfonates and is regulated by the transcriptional activator Cbl. *J. Biol. Chem.* **1999**, *274*, 29358−29365.
(6) Kahnert, A.; Vermeij, P.; Wietek, C.; James, P.; Leisinger, T.; Kertesz, M. A. The ssu locus plays a key role in organosulfur metabolism in *Pseudomonas putida* S-313. *J. Bacteriol.* **2000**, *182*, 2869−2878.
(7) Kertesz, M. A.; Schmidt-Larbig, K.; Wüest, T. A novel reduced flavin mononucleotide-dependent methanesulfonate sulfonatase encoded by the sulfur-regulated msu operon of *Pseudomonas aeruginosa*. *J. Bacteriol.* **1999**, *181*, 1464−1473.
(8) Soule, J.; Gnann, A. D.; Gonzalez, R.; Parker, M. J.; McKenna, K. C.; Nguyen, S. V.; Phan, N. T.; Wicht, D. K.; Dowling, D. P. Structure and function of the two-component flavin-dependent methanesulfinate monooxygenase within bacterial sulfur assimilation. *Biochem. Biophys. Res. Commun.* **2020**, *522*, 107−112.
(9) Wicht, D. K. The reduced flavin-dependent monooxygenase SfnG converts dimethylsulfone to methanesulfinate. *Arch. Biochem. Biophys.* **2016**, *604*, 159−166.
(10) Driggers, C. M.; Dayal, P. V.; Ellis, H. R.; Karplus, P. A. Crystal structure of *Escherichia coli* SsuE: defining a general catalytic cycle for FMN reductases of the flavodoxin-like superfamily. *Biochemistry* **2014**, *53*, 3509−3519.
(11) Fodje, M. N.; Al-Karadaghi, S. Occurrence, conformational features and amino acid propensities for the pi-helix. *Protein Eng.* **2002**, *15*, 353−358.
(12) Cooley, R. B.; Arp, D. J.; Karplus, P. A. Evolutionary Origin of a Secondary Structure: π-Helices as Cryptic but Widespread Insertional Variations of α-Helices That Enhance Protein Functionality. *J. Mol. Biol.* **2010**, *404*, 232−246.
(13) Weaver, T. M. The π-helix translates structure into function. *Protein Sci.* **2008**, *9*, 201−206.
(14) Tu, S. C.; Lei, B.; Liu, M.; Tang, C. K.; Jeffers, C. Probing the mechanisms of the biological intermolecular transfer of reduced flavin. *J. Nutr.* **2000**, *130*, 331S−332S.
(15) Jeffers, C. E.; Nichols, J. C.; Tu, S. C. Complex formation between *Vibrio harveyi* luciferase and monomeric NADPH:FMN oxidoreductase. *Biochemistry* **2003**, *42*, 529−534.
(16) Abdurachim, K.; Ellis, H. R. Detection of protein-protein interactions in the alkanesulfonate monooxygenase system from *Escherichia coli*. *J. Bacteriol.* **2006**, *188*, 8153−8159.
(17) Dayal, P. V.; Singh, H.; Busenlehner, L. S.; Ellis, H. R. Exposing the Alkanesulfonate Monooxygenase Protein-Protein Interaction Sites. *Biochemistry* **2015**, *54*, 7531−7538.
(18) Jun, S. Y.; Lewis, K. M.; Youn, B.; Xun, L.; Kang, C. Structural and biochemical characterization of EDTA monooxygenase and its physical interaction with a partner flavin reductase. *Mol. Microbiol.* **2016**, *100*, 989−1003.
(19) Li, H.; Forson, B.; Eckshtain-Levi, M.; Valentino, H.; Martín Del Campo, J. S.; Tanner, J. J.; Sobrado, P. Biochemical Characterization of the Two-Component Flavin-Dependent Monooxygenase Involved in Valanimycin Biosynthesis. *Biochemistry* **2021**, *60*, 31−40.
(20) Gao, B.; Ellis, H. R. Altered mechanism of the alkanesulfonate FMN reductase with the monooxygenase enzyme. *Biochem. Biophys. Res. Commun.* **2005**, *331*, 1137−1145.
(21) McFarlane, J. S.; Hagen, R. A.; Chilton, A. S.; Forbes, D. L.; Lamb, A. L.; Ellis, H. R. Not as easy as π: An insertional residue does not explain the π-helix gain-of-function in two-component FMN reductases. *Protein Sci.* **2019**, *28*, 123−134.
(22) Schuck, P. Size-distribution analysis of macromolecules by sedimentation velocity ultracentrifugation and lamm equation modeling. *Biophys. J.* **2000**, *78*, 1606−1619.
(23) Jumper, J.; Evans, R.; Pritzel, A.; Green, T.; Figurnov, M.; Ronneberger, O.; Tunyasuvunakool, K.; Bates, R.; Žídek, A.; Potapenko, A.; Bridgland, A.; Meyer, C.; Kohl, S. A. A.; Ballard, A. J.; Cowie, A.; Romera-Paredes, B.; Nikolov, S.; Jain, R.; Adler, J.; Back, T.; Petersen, S.; Reiman, D.; Clancy, E.; Zielinski, M.; Steinegger, M.; Pacholska, M.; Berghammer, T.; Bodenstein, S.; Silver, D.; Vinyals, O.; Senior, A. W.; Kavukcuoglu, K.; Kohli, P.; Hassabis, D. Highly accurate protein structure prediction with AlphaFold. *Nature* **2021**, *596*, 583−589.
(24) Schrödinger, LLC. *The PyMOL Molecular Graphics System*, Version 1.8, 2015.
(25) Li, B.; Lin, S. X. Fluorescence-Energy Transfer in Human Estradiol 17beta-Dehydrogenase-NADPH Complex and Studies on the Coenzyme Binding. *Eur. J. Biochem.* **1996**, *235*, 180−186.
(26) James, E. I.; Murphree, T. A.; Vorauer, C.; Engen, J. R.; Guttman, M. Advances in hydrogen/deuterium exchange mass spectrometry and the pursuit of challenging biological systems. *Chem. Rev.* **2022**, *122*, 7562−7623.
(27) Sitkiewicz, E.; Tarnowski, K.; Poznański, J.; Kulma, M.; Dadlez, M. Oligomerization interface of RAGE receptor revealed by MS-monitored hydrogen deuterium exchange. *PLoS One* **2013**, *8*, No. e76353.
(28) Dautant, A.; Meyer, P.; Georgescauld, F. Hydrogen/deuterium exchange mass spectrometry reveals mechanistic details of activation of nucleoside diphosphate kinases by oligomerization. *Biochemistry* **2017**, *56*, 2886−2896.
(29) Illes-Toth, E.; Meisl, G.; Rempel, D. L.; Knowles, T. P. J.; Gross, M. L. Pulsed hydrogen-deuterium exchange reveals altered structures and mechanisms in the aggregation of familial alzheimer's disease mutants. *ACS Chem. Neurosci.* **2021**, *12*, 1972−1982.
(30) Polakowska, M.; Steczkiewicz, K.; Szczepanowski, R. H.; Wysłouch-Cieszyńska, A. Toward an understanding of the conformational plasticity of S100A8 and S100A9 Ca^{2+}-binding proteins. *J. Biol. Chem.* **2023**, *299*, 102952.
(31) Frieden, C. Protein oligomerization as a metabolic control mechanism: Application to apoE. *Protein Sci.* **2019**, *28*, 837−842.
(32) Levy, E. D.; Teichmann, S. Structural, evolutionary, and assembly principles of protein oligomerization. *Progress in Molecular Biology and Translational Science*; Elsevier, 2013; Vol. *117*, pp 25−51.
(33) Marsh, J. A.; Teichmann, S. A. Structure, dynamics, assembly, and evolution of protein complexes. *Annu. Rev. Biochem.* **2015**, *84*, 551−575.
(34) Liu, M.; Lei, B.; Ding, Q.; Lee, J. C.; Tu, S. C. Vibrio harveyi NADPH:FMN oxidoreductase: preparation and characterization of the apoenzyme and monomer-dimer equilibrium. *Arch. Biochem. Biophys.* **1997**, *337*, 89−95.
(35) Kendrew, S. G.; Harding, S. E.; Hopwood, D. A.; Marsh, E. N. Identification of a Flavin:NADH Oxidoreductase Involved in the Biosynthesis of Actinorhodin. *J. Biol. Chem.* **1995**, *270*, 17339−17343.
(36) Liew, J. J. M.; El Saudi, I. M.; Nguyen, S. V.; Wicht, D. K.; Dowling, D. P. Structures of the alkanesulfonate monooxygenase MsuD provide insight into C-S bond cleavage, substrate scope, and an unexpected role for the tetramer. *J. Biol. Chem.* **2021**, *297*, 100823.
(37) Musila, J. M.; Ellis, H. R. Transformation of a flavin-free FMN reductase to a canonical flavoprotein through modification of the π-helix. *Biochemistry* **2016**, *55*, 6389−6394.
(38) Musila, J. M.; L Forbes, D.; Ellis, H. R. Functional evaluation of the π-helix in the NAD(P)H:FMN reductase of the alkanesulfonate monooxygenase system. *Biochemistry* **2018**, *57*, 4469−4477.
(39) Sazinsky, M. H.; Lippard, S. J. Product bound structures of the soluble methane monooxygenase hydroxylase from *Methylococcus capsulatus* (Bath): protein motion in the alpha-subunit. *J. Am. Chem. Soc.* **2005**, *127*, 5814−5825.
(40) Zhan, X.; Carpenter, R. A.; Ellis, H. R. Catalytic importance of the substrate binding order for the $FMNH_2$-dependent alkanesulfonate monooxygenase enzyme. *Biochemistry* **2008**, *47*, 2221−2230.
(41) Sucharitakul, J.; Phongsak, T.; Entsch, B.; Svasti, J.; Chaiyen, P.; Ballou, D. P. Kinetics of a two-component p-hydroxyphenylacetate hydroxylase explain how reduced flavin is transferred from the reductase to the oxygenase. *Biochemistry* **2007**, *46*, 8611−8623.
(42) Bradshaw, M. D.; Gaffney, B. J. Fluctuations of an exposed π-helix involved in lipoxygenase substrate recognition. *Biochemistry* **2014**, *53*, 5102−5110.

https://doi.org/10.1021/acs.biochem.3c00361
Biochemistry 2023, 62, 2751−2762